

Homological analysis of multi-qubit entanglement

Alessandra Di Pierro^{*}, Stefano Mancini[†], Laleh Memarzadeh[‡], Riccardo Mengoni[§]

¹Department of Informatics, University of Verona, Strada Le Grazie 15, 37134 Verona, Italy

²School of Science and Technology, University of Camerino, I-62032 Camerino, Italy

³INFN-Sezione di Perugia, I-06123 Perugia, Italy

⁴Department of Physics, Sharif University of Technology, Teheran, Iran

We propose the usage of persistent homologies to characterize multipartite entanglement. On a multi-qubit data set we introduce metric-like measures defined only in terms of bipartite entanglement and then we derive barcodes. We show that they are able to provide a good classification of entangled states, at least for a small number of qubit.

PACS numbers: 03.67.Mn, 02.40.Re, 02.70.-c

I. INTRODUCTION

In the last few decades the interest on quantum entanglement has been turned from purely foundational/philosophical aspects to more practical/applicative ones, thanks to quantum information processing. Along this line entanglement characterization becomes of uppermost importance, although it results a daunting task in multi-partite systems. Many approaches have been developed, based on combinatorics, group theory, geometry, etc. (see e.g. [1] for a review). However topological approaches have been almost untaken.

Persistent homology is nowadays widely used to analyse classical data sets represented in the form of *point cloud* [2]. It is a particular sampling based technique from algebraic topology, originally introduced in [3], aiming at extracting coarse topological information from high dimensional data sets.

A quantum approach to compute persistent homology has been devised in order to achieve more efficient algorithms for classical data analysis [4], but viceversa the usage of persistent homologies in quantum data set has not been pursued. Here we propose persistent homologies for characterizing multipartite entanglement. On a multi-qubit data set we introduce metric-like measures only based on bipartite entanglement and then derive barcodes. We show that they are able to provide a good classification of entangled states, at least for a small number of qubit.

II. PERSISTENT HOMOLOGY IN A NUTSHELL

Information about topological properties of a topological space X , such as connected components, holes, voids etc., are encoded in the homology groups $\{H_0(X), H_1(X), H_2(X), \dots\}$ of the space X , where the k^{th} homology group $H_k(X)$ describes the k -dimensional holes in X [5].

In order to capture the global topological features in a data set, the corresponding space must first be represented as a simplicial complex. There are different ways for assigning such simplicial complexes to the data points but all methods are based on distances ϵ between pairs of the points. Fixing the method, by changing ϵ , different topological features (such as connected components, tunnels, voids etc. detected by homology) are observed in the global complex. Hence varying ϵ from small values to sufficiently large ones enables us to find which topological features persists and hence are important. This method of computing multi-scale homological features of the data points is called persistent homology. Those features which vanish by changing the parameter ϵ , are considered as noise with no particular significance.

Here we focus on the Rips complex [9] to construct simplicial complexes from data points [6]. In the Rips complex, k -simplices correspond to $(k+1)$ points which are pairwise within distance ϵ . Computing topological features for the whole range of ϵ , we produce a barcode, i.e. a collection of horizontal lines in a plane where the horizontal axis represents ϵ while on the vertical axis the homology generators H_k are placed in arbitrary order.

Hereafter, a black line in the barcode will indicate a connected component (homology group H_0), a red line will correspond to a hole (homology group H_1) and a blue line will represent a void (homology group H_2).

III. SEMI-METRICS ON QUANTUM DATA SET

Consider a quantum dataset \mathcal{Q} representing a quantum state $|\Psi_n\rangle$ over n qubit as a point cloud. This dataset is such that to each point in \mathcal{Q} is associated a single qubit. Let $E(i, j)$ be an entanglement monotone between qubit i and j . Our aim is to define a metric on \mathcal{Q} in such a way that the more entangled two qubit are, the closer they are with respect to that metric. This naturally leads to define a distance as follows:

$$D(i, j) := [E(i, j)]^{-1}, \quad (1)$$

with $D(i, j) = 0$ iff $i = j$. However, this does not define a proper metric but a semi-metric because the triangle inequality does not hold.

^{*}email: alessandra.dipierro@univr.it

[†]email: stefano.mancini@unicam.it

[‡]email: memarzadeh@sharif.edu

[§]email: riccardo.mengoni@univr.it

Since $D(i, j)$ only takes into account bipartite entanglement between pairs of qubits and no other form of entanglement, we introduce a variant of $D(i, j)$ that includes bipartite entanglement between any possible pair of subsets containing qubit i and j as:

$$\tilde{D}(i, j) = \prod_{k=0}^{n-2} \prod_{S_k \in \mathcal{P}_k} E(S_k \cup i, \bar{S}_k \cup j), \quad (2)$$

where $\mathcal{P}_k = \{S \subseteq \{1..n\} \setminus \{i, j\} \text{ s.t. } |S| = k\}$ is the set of all the subsets S_k containing k elements in $\{1..n\} \setminus \{i, j\}$ and \bar{S}_k is the complement of S_k .

It is clear that also $\tilde{D}(i, j)$ is a semi-metric because likewise $D(i, j)$ it does not satisfy the triangle inequality.

IV. CLASSIFICATION OF QUBIT STATES

For three qubit, Equation (2) becomes

$$\tilde{D}(i, j) := \left[E(i, j) + E(i, \{j, k\})E(j, \{i, k\}) \right]^{-1} \quad (3)$$

with $i \neq j \neq k$. Using this distance, it is possible to distinguish between the following macro-classes of states.

1) Fully separable states

Pure states of this kind are not entangled and can be written as $|\psi_1\rangle|\psi_2\rangle|\psi_3\rangle$ where $|\psi_i\rangle$ is a generic state for qubit i . In this case, whatever labelling i, j, k of the three qubits, we get $E(i, j) = 0 \forall i, j$ and $E(i, \{j, k\}) = E(j, \{i, k\}) = 0$. This means that $\tilde{D}(i, j) = \infty$ for every pair of qubits. The point cloud associated to this state is made up of three points placed at infinite distance from each other, hence the barcode associated is the one shown in Figure 1.

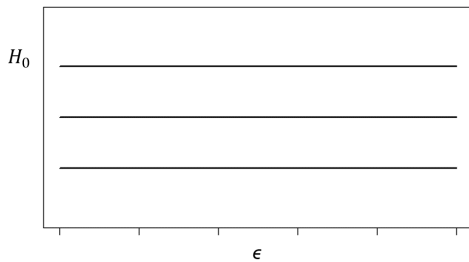


Figure 1: Barcode for three qubit fully separable states.

2) Bi-separable states

Pure states of this kind can be written as $|\psi_i\rangle|\psi_{jk}\rangle$ where $|\psi_{jk}\rangle$ is an entangled states between qubit j and k . In this case we get $E(i, j) = E(i, k) = 0$ and $E(j, k) \neq 0$, while $E(i, \{j, k\}) = 0$ but $E(j, \{i, k\}) \neq 0$ as well as $E(k, \{i, j\}) \neq 0$. This means that $\tilde{D}(i, j) = \tilde{D}(i, k) = \infty$ but $\tilde{D}(j, k) < \infty$. Hence the resulting barcode is as in Figure 2.

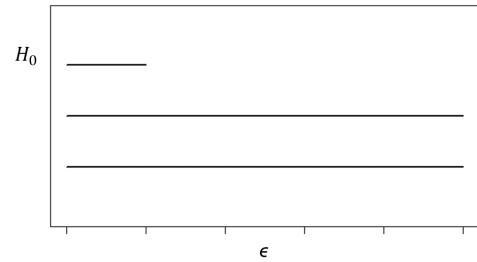


Figure 2: Barcode for three qubit bi-separable states.

3) Fully inseparable states Pure states of this kind can only be written as $|\psi_{123}\rangle$ i.e. as an entangled three qubit state.

Examples of this kind of states are the GHZ state

$$|GHZ_{123}\rangle = \frac{1}{\sqrt{2}} (|000\rangle + |111\rangle), \quad (4)$$

and the W state

$$|W_{123}\rangle = \frac{1}{\sqrt{3}} (|100\rangle + |010\rangle + |001\rangle). \quad (5)$$

Although similar in the associated barcode, these two states have different characteristics. In the GHZ state we get $E(i, j) = 0, \forall i, j$, but both $E(i, \{j, k\})$ and $E(j, \{i, k\})$ differ from zero $\forall i, j, k$. This means that $0 < \tilde{D}(i, j) < \infty, \forall i, j$, and the three points in the point cloud are at finite distance from each other. In the W state instead, we get $E(i, j) \neq 0 \forall i, j$ and this is enough to ensure that $0 < \tilde{D}(i, j) < \infty \forall i, j$. Thus, also in this case the three points in the point cloud are at finite distance from each other.

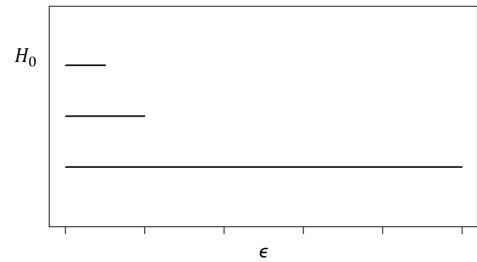


Figure 3: Barcode for three qubit fully inseparable states.

In summary all fully inseparable states give barcodes similar to the one depicted in Figure 3, which however may differ in the length of the first two lines depending on the characteristics of the state.

For four qubit states, Equation (2) becomes

$$\begin{aligned} \tilde{D}(i, j) = & \left[E(i, j) + E(i, \{j, k, l\})E(j, \{i, k, l\}) \right. \\ & \times E(\{j, l\}, \{i, k\})E(\{j, k\}, \{i, l\}) \left. \right]^{-1} \end{aligned} \quad (6)$$

with $i \neq j \neq k \neq l$. In a similar way as shown for the three qubit case, it is possible to distinguish between the following macro-classes:

1') states that are fully separable ($|\psi_1\rangle|\psi_2\rangle|\psi_3\rangle|\psi_4\rangle$) have associated the barcode as in Figure 4;

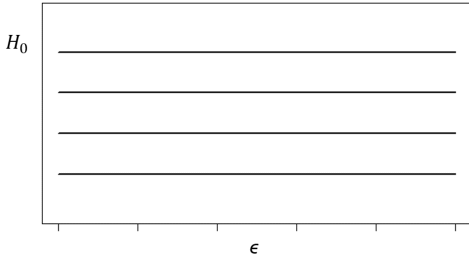


Figure 4: Barcode for four qubit fully separable states.

2') states that are tri-separable (e.g. $|\psi_1\rangle|\psi_2\rangle|\psi_{34}\rangle$) have associated the barcode as in Figure 5;

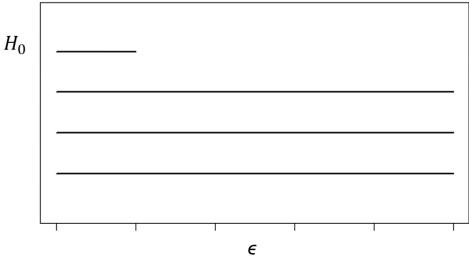


Figure 5: Barcode for four qubit tri-separable states.

3') states that are bi-separable (e.g. $|\psi_1\rangle|\psi_{234}\rangle$) have associated the barcode in Figure 6;

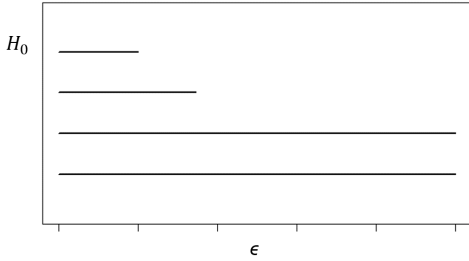


Figure 6: Barcode for four qubit bi-separable states.

4') states that are fully inseparable ($|\psi_{1234}\rangle$) are all mapped to point clouds whose four points are at finite distance from each another. States of this macro-class could have associated one of the two barcodes shown in Figure 7. The bottom barcode has a hole (red line) for a small interval of the distance: its presence depends on the particular values that (6) may have, but it does not add any information to the classification.

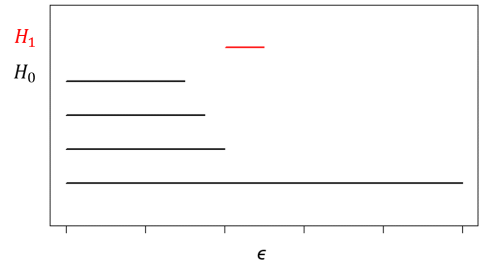
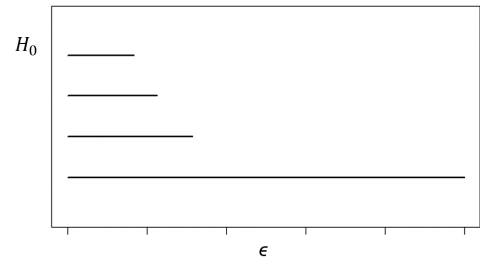


Figure 7: Barcodes for four qubit fully inseparable states.

V. NESTED CLASSIFICATION OF QUBIT STATES

In the previous section we provided a classification of multi-qubit states in macro-classes. It may happen that a single macro-class is composed by several sub-classes. Then the problem arises of whether or not a more refined classification is possible by means of barcodes. We shall show that this can simply be done by resorting to the distance (1).

In the case of three qubit states, the fully inseparable macro-class 3) splits into the subclasses listed below. In order to visually distinguish them we draw the graph obtained from the point cloud when ϵ is larger than the maximum distance $D(i, j)$ between pairs of qubit. We use the same colour for those nodes that represent qubits sharing full multipartite entanglement.

a) This subclass has $|GHZ\rangle$ as a representative and gathers all those states where entanglement between any possible pair of the three qubits gives $E(i, j) = 0, \forall i, j$. This implies that each one of the three points of our point cloud is infinitely far away from the others. Hence they generate a barcode that only displays the 0-order homology group H_0 , i.e the connected components as shown in Figure 8.

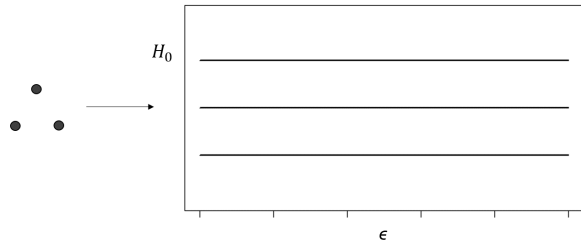


Figure 8: Barcode for three qubit states a)

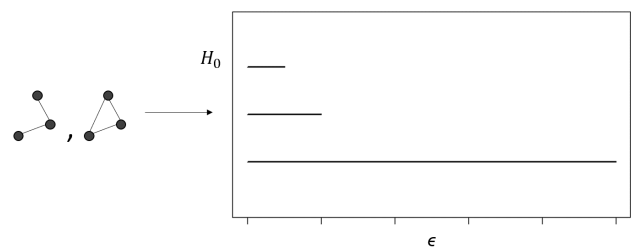


Figure 10: Barcode for three qubit states c)

b) Another subclass is defined by states where $E(i, j) > 0$, $E(j, k) = 0$ and $E(i, k) = 0$; the associated point cloud is made of three points where the first and the second are at a finite distance, while the third point is at infinite distance from the other two. The barcode shows three different connected components in the interval $[0, \frac{1}{E(i,j)}]$, while for values greater than $\frac{1}{E(i,j)}$ only two of them persist as shown in Figure 9.

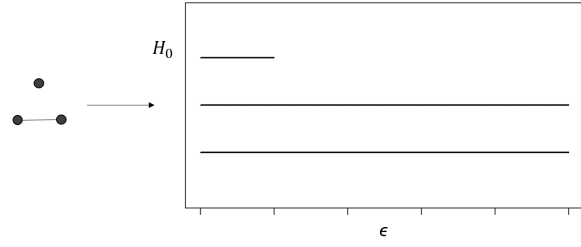
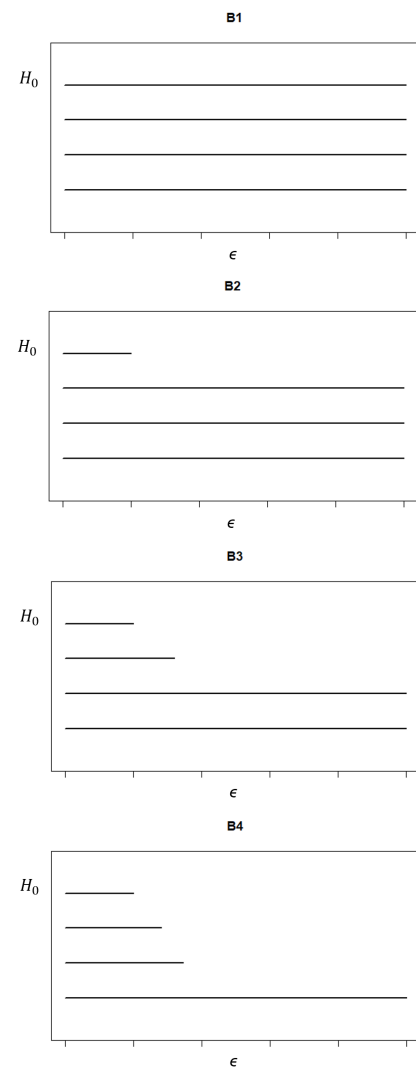


Figure 9: Barcode for three qubit states b)

c) This subclass contains two kinds of states with different characteristics. States of the first kind have $E(i, j), E(j, k) > 0$ and $E(i, k) = 0$; the associated point cloud is made of three points where the first and the second are at distance $\frac{1}{E(i,j)}$, the second and the third are at distance $\frac{1}{E(j,k)}$, but the first and the third points are at infinite distance. This can be seen in the barcode of Figure 10 where two of the three lines vanish and only one persists.

For states of the second kind, i.e. W-like states, at a finite value ϵ^* of $D(i, j)$ the three points get connected one to each other to form a triangular graph that is immediately filled with a 2-simplex. This means that for $\epsilon \geq \epsilon^*$ we are left with only one connected component (the 2-simplex), again shown by the barcode of Figure 10.

For states of four qubits we can identify sub-classes in the case of states belonging to 3') and 4'). The results obtained using the distance (1) are summarised in Table I, which refers to barcodes of Figure 11.



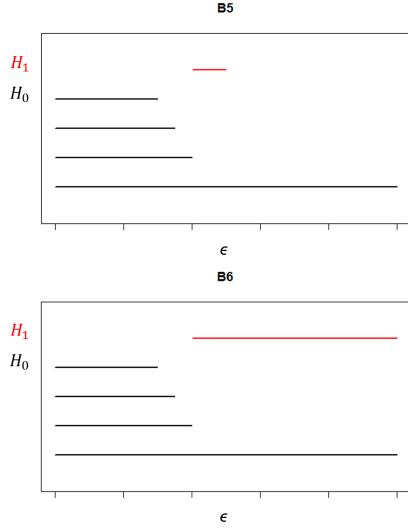


Figure 11: Four qubit barcodes B1-B6

Note that for states 4'k) the barcode may be of B4 or B5 type depending on the strength of the pairwise entanglement between qubits.

In both three and four qubit cases, we observe that the usage of (1) does not allow us to resolve all sub-classes. An improvement can be obtained by using a different kind of complex as explained in the following section.

VI. RIPS VS ČECH COMPLEX

The Rips complex is closely related to another simplicial complex, called the Čech complex. This is defined on a set of balls and has a simplex for every finite subset of balls with nonempty intersection; thus, while in Rips complexes, k -simplices correspond to $(k+1)$ points which are pairwise within distance ϵ , in Čech complexes k -simplices are determined by $(k+1)$ points whose closed $\epsilon/2$ -ball neighborhood have a point of common intersection [8].

By the Čech theorem [7], the Čech complex has the same topological structure as the open sets (ϵ -balls) cover of the point cloud. This is not true for the Rips complex, which is more coarse than the Čech complex. Therefore, the latter is a more powerful tool for classification with respect to Rips. In fact, it is possible to refine the classification of the three qubit states in class 3). The reason why this is possible is that in the Čech complex, triangle graphs like the one that appears in the W-like state point cloud (Figure 10) are not immediately filled with a 2-simplex. In fact a hole (1-order homology group H_1) appears for a short interval of the distance $\frac{1}{E(i,j)}$ before the graph gets filled with the 2-simplex.

Therefore, while the barcode for states of the first type in c) remains the same as in Figure 10, the one for the W-like states becomes as shown in Figure 12.

| Macroclass | State | Barcode |
|-----------------------|-------|----------|
| 3') Bi-separable | a) | B1 |
| 3') | b) | B2 |
| 3') | c) | B3 |
| 3') | d) | B3 |
| 3') | e) | B3 |
| 4') Fully inseparable | a) | B1 |
| 4') | b) | B2 |
| 4') | c) | B3 |
| 4') | d) | B3 |
| 4') | e) | B3 |
| 4') | f) | B4 |
| 4') | g) | B4 |
| 4') | h) | B4 |
| 4') | i) | B6 |
| 4') | j) | B4 |
| 4') | k) | B4 or B5 |

Table I: Classification of four qubit states 3') and 4').

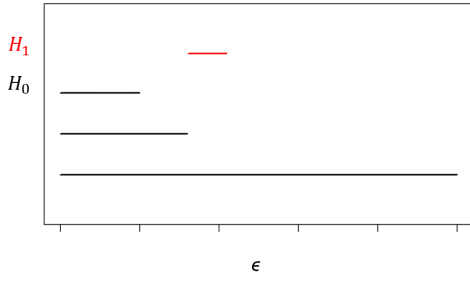


Figure 12: Barcode for W-like states with Čech complex.

Analogously, the Čech complex allows us to refine the classification of states 3'c), 3'd) and 3'e). In fact 3'd) will now have barcode B7 shown in Figure 13. For the class 4') of fully inseparable states, we can obtain the improvement shown in Table II and Figure 13:

VII. CONCLUSION

We have proposed the use of persistent homologies to study multi-partite entanglement. The analysis we have shown, although being a topological analysis gathering as such only qualitative information, turns out to be quite powerful (at least for small number of qubit), since it can recognize all macro-classes of states and for nested application also most of the sub-classes.

For an extension of the approach to very large quantum data sets one has to deal with the exponential complexity of Equation (2) which implies the calculation of $\frac{n(n-1)}{2}2^{n-2}$ correlation measures; these would reduce to the more tractable number of $\frac{n(n-1)}{2}$ if we used Equation (1). Hence future investigations should seek a more efficient distance-like measure which is still able to capture relevant features of classes of states. Efforts in this direction should be combined with the investigation of true metrics (rather than just semi-metrics) on the quantum data set, based on bi-partite entanglement measures.

We believe that the presented work paves the way to the cross fertilization of apparently distant fields like big data analysis and quantum entanglement.

| Macroclass | State | Rips barcode | Čech barcode |
|------------|-------|--------------|--------------|
| 4') | a) | B1 | B1 |
| 4') | b) | B2 | B2 |
| 4') | c) | B3 | B3 |
| 4') | d) | B3 | B3 |
| 4') | e) | B3 | B7 |
| 4') | f) | B4 | B4 |
| 4') | g) | B4 | B4 |
| 4') | h) | B4 | B5 |
| 4') | i) | B6 | B6 |
| 4') | j) | B4 | B8 |
| 4') | k) | B4/B5 | B9 |

Table II: Comparison between barcodes obtained from the Rips and Čech complex for states belonging to the class 4')

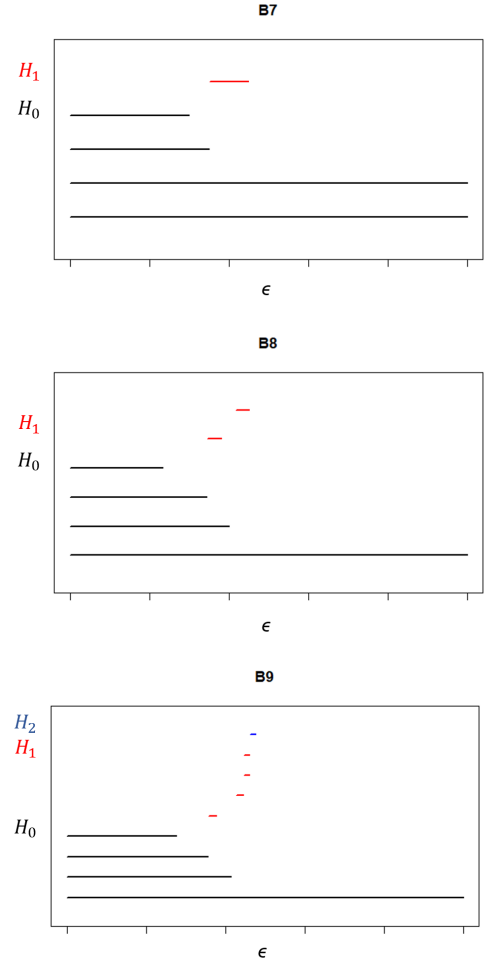


Figure 13: Four qubit barcode B7-B9.

- [1] Horodecki R., et al., *Rev. Mod. Phys.* **81**, 865 (2009).
- [2] Carlsson G. and Zomorodian A, *Discrete Comput. Geom.*, **33**, 249 (2005).
- [3] Edelsbrunner H., Letscher D., and Zomorodian A., *Discrete Comput. Geom.*, **28**, 511 (2002).
- [4] Lloyd S., Garnerone S., and Zanardi P., arXiv:1408.3106 [quant-ph] (2014).
- [5] Hatcher, A., Cambridge University Press. (2002).
- [6] Carlsson, E. et al., *Int. J. Comput. Geom. Appl.*, **16**, 291 (2006).
- [7] Borsuk K., *Fundamenta Mathematicae*, **35**(1):217–234 (1948).
- [8] Ghrist, R. *Bulletin of the American Mathematical Society*, Vol. 45(2008)
- [9] Most commonly known as Vietoris-Rips complex, here we will call it Rips complex for the sake brevity.